EUROPEAN COMMISSION

European Research Area

SKIN Project

Work Package 4: Modeling, Theory

Task 4.1: Approaches to Model the Kinetics of Trace Element Uptake in Host Minerals

DELIVERABLE D4.1

PRELIMINARY REVIEW ON MODELING APPROACHES AND THEIR IMPLEMENTATION

COLLABORATIVE PROJECT (CP)

Grant agreement N°269688

Submitting organizations: PSI

Author(s): Bruno Thien, Dmitrii A. Kulik, Enzo Curti

Due date of deliverable: Month 18

Actual submission: Month 20

Start date of the project: 01 January 2011

Duration: 36 months

Project co-funded by the European Commission under the Seventh Framework Programme of the European Atomic Energy Community (Euratom) for nuclear research and training activities (2007 to 2011)		
Dissemination Level		
PU	Public	
RE	Restricted to a group specified by the partners of the project	X
CO	Confidential, only for partners of the project	

This page is intentionally left blank

Abstract

Trace element partitioning between a host mineral and the aqueous solution often depends on mineral growth rates and is frequently irreversible, as seen from the experimental data and the occurrence of zoned crystals. Kinetically dependent trace element uptake can be realistically simulated using thermodynamic models that describe partial equilibria between aqueous and solid solution with simultaneous account of fast (instantaneous) surface adsorption. In such a reaction-path sequence, the aqueous phase is in full thermodynamic equilibrium only with part of the solids, implying that some amounts of relevant phases, end members, or adsorbed species must be declared metastable according to time-dependent kinetic rate laws.

In this context, we considered three uptake kinetics models from the literature: the growth Surface Entrapment Model (SEMO), the Surface Reaction Kinetic Model (SRKM), and the Adsorption – Diffusion -Desorption Model (ADDM). Each model predicts a final metastable solid-aqueous distribution of trace elements or isotopes. However, different mechanisms are invoked: the competition between mineral growth and near-surface diffusivity (SEMO); purely kinetic laws for gross forward and backward reaction rates for host and trace components (SRKM); or diffusion of trace component into the solid (ADDM). Each model can adequately describe the trace element uptake for single element/host mineral pairs (e.g. Sr/calcite, Cd/calcite) under simplifying assumptions, such as the constancy of the growth rate and of the aqueous composition.

Our analysis shows that SEMO and SRKM models can be merged in a simple ‘generalized’ model suitable for geochemical reactive transport simulations. The merged model was implemented in the GEM-Selektor code as iterative script that controls time step- dependent metastability constraints on the amounts of the solid solution, host- and trace end members in the Gibbs energy minimization algorithm. This tool can also account for changes in solid and aqueous chemistry that may occur upon the uptake in a closed system (e.g. from pore solution), while keeping track of surface areas of minerals during growth or dissolution.

Table of Contents

1. Introduction: Context of the study

The objective of Task 4.1 is to develop a new partial equilibrium approach to geochemical modeling of the slow uptake of radionuclides upon (re)precipitation of host-mineral solid solutions (SS)).Irreversible trace element uptake in growing minerals cannot be accurately predicted using an equilibrium aqueous solid-solution thermodynamic model alone because the experimentally measured trace element partitioning usually depends on precipitation rates and related kinetic effects (Fig. 1). A suitable model has to account for such deviations from 'true' equilibrium. In this contribution, three existing models of trace element uptake in host minerals that take into account kinetic effects were evaluated and compared: the Surface (growth) Entrapment Model (SEMO) (Watson, 2004; Watson and Liang, 1995), the Surface Reaction Kinetic Model (SRKM) (DePaolo, 2011), and the Adsorption Diffusion Desorption Model (ADDM) (Barrow, 1983).

To succeed in predicting trace elements uptake in (growing) minerals, some questions must be answered first. Why does trace element uptake depend on precipitation (re-crystallization) rates, as revealed by many experiments? What are the mechanisms controlling this phenomenon? What is the trace element distribution in thermodynamic equilibrium, as a reference for the kinetically-dependent uptake?

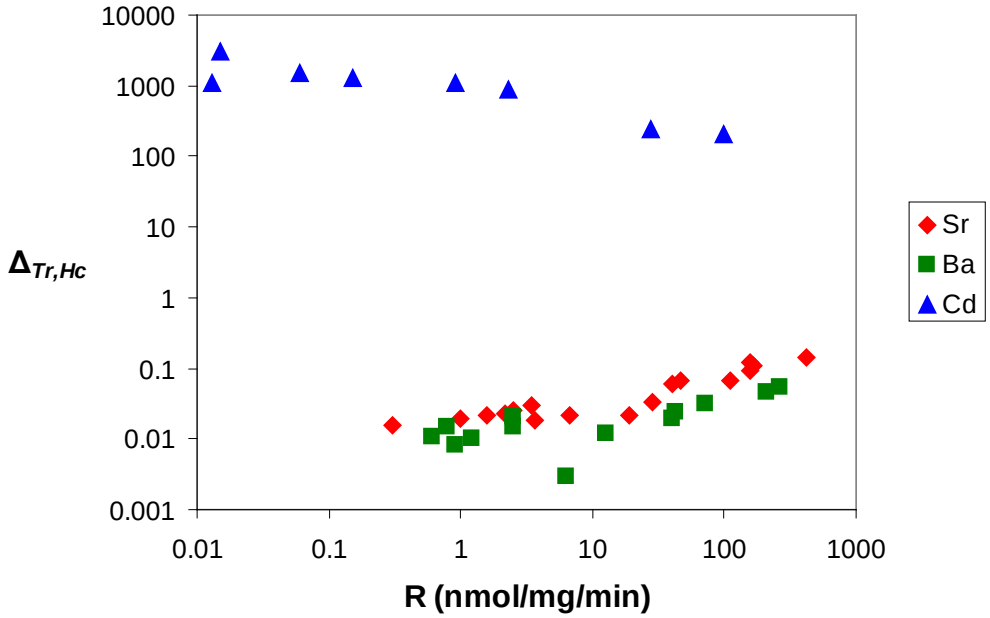

Fig.1: Fractionation coefficient (see section 2 for explanations) of Sr, Ba and Cd in calcite as a function of growth rate. Data from Tesoriero and Pankow (1996). $\Delta_{Cd,Ca}$ values are much higher than $\Delta_{Sr,Ca}$ and $\Delta_{Ba,Ca}$ showing that Cd is more easily incorporated in calcite than Sr or Ba. This is the expected behaviour because the ionic radius of Cd^{2+} is slightly smaller than that of Ca^{2+} and the ionic charge is identical. Ions like Cd^{2+}, and to less extent $Co^{2+,}$ Fe^{2+}, Mn^{2+}, Ni^{2+} are called "compatible" with calcite by virtue of their size and charge properties. On the other hand, Sr^{2+} and Ba^{2+} have much greater ionic radii than Ca^{2+}, hence it should be more difficult to accommodate these ions within the calcite structure; these ions are called "incompatible". Compatible and incompatible trace elements exhibit different behaviours. $\Delta_{Cd,Ca}$ decreases when the precipitation rate increases, whereas $\Delta_{Sr,Ca}$ and $\Delta_{Ba,Ca}$ increase when the precipitation rate increases.

2. Models and methods

Because of the diversity of possible conditions, the empirical prediction of trace element partitioning between aqueous phase and minerals would require a very large number of laboratory experiments, the maximum duration of which is still very short in comparison with time scales relevant in the waste disposal context. That is why models must be developed, at best based on a "mechanistic" process understanding. Unfortunately, the involved phenomena are only partially known; more experimental data is necessary to validate uptake mechanisms and to constrain their relevant parameters.

2.1. Fractionation coefficient

The distribution of a trace element *Tr* between the aqueous solution (or melt) and the mineral (crystalline solid solution) relative to the host component *Hc* is usually described by the fractionation coefficient $\Delta_{Tr,Hc}$, which is the ratio of two distribution ratios *Rd:*

$$\Delta_{Tr,Hc} = \frac{Rd(Tr)}{Rd(Hc)} \tag{2-1}$$

Distribution ratio is defined as the ratio of component concentration in the solid to that in the aqueous phase. Taking mole fraction *x* for the solid and molarity [] or molality for the aqueous part, equation (2-1) can be rewritten as follows:

$$\Delta_{Tr,Hc} = \left(\frac{x_{Tr}}{[Tr]}\right) \Big/ \left(\frac{x_{Hc}}{[Hc]}\right) \tag{2-2.a}$$

This equation is most frequently used in the re-arranged form:

$$\Delta_{Tr,Hc} = \frac{x_{Tr}}{x_{Hc}} \cdot \frac{[Hc]}{[Tr]} \tag{2-2.b}$$

$\Delta_{Tr,Hc}$ can be related to a thermodynamic constant of an exchange reaction, for instance Sr incorporation in calcite:

$$Sr^{2+} + CaCO_3 \Leftrightarrow Ca^{2+} + SrCO_3 \tag{2-3}$$

The equilibrium fractionation (exchange) constant of this reaction is:

$${}^{\Delta}K_{Sr,Ca,eq} = \frac{x_{SrCO_3}\gamma_{SrCO_3}}{x_{CaCO_3}\gamma_{CaCO_3}} \cdot \frac{[Ca^{2+}]\cdot\gamma_{Ca^{2+}}}{[Sr^{2+}]\cdot\gamma_{Sr^{2+}}} \tag{2-4}$$

where γ stand for the activity coefficients. Comparing eqs (2-2) and (2-4) one can see that, assuming the same extent of complexation of Ca^{2+} and Sr^{2+} aqueous ions,

$${}^{\Delta}K_{Sr,Ca} \approx \Delta_{Sr,Ca} \frac{\gamma_{Sr,ss}}{\gamma_{Ca,ss}} \frac{\gamma_{Ca,aq}}{\gamma_{Sr,aq}} \tag{2-5}$$

both in equilibrium and in metastable state. In the case of very dilute aqueous electrolyte and ideal solid solution (ss), eq (2-5) further simplifies to ${}^{\Delta}K_{Tr,Hc} \approx \Delta_{Tr,Hc}$.

2.2. Growth (Surface) Entrapment Model (SEMO)

The first version of the Growth Entrapment Model was originally proposed by Watson and Liang (1995) and later improved by Watson (2004) to account for the surface depletion of some elements and the depth variability of the diffusivity in calcite (Watson, 2004). The starting point of this model was the frequent observation of zoning in slowly-growing magmatic minerals like monazite or zircon.

The main assumption of SEMO is: "*a growing crystal takes the composition of its surface, unless diffusivity in a thin near-surface region is effective during growth*." In other words, there is a competition between precipitation rate and diffusivity. In general, the equilibrium concentration of a trace element adsorbed on the mineral surface will be different than its concentration in solid solution in equilibrium with the same aqueous electrolyte phase. If mineral growth is faster than the diffusion of the trace element within the few nanometre-thick layers beneath the mineral surface, the bulk solid will partly "inherit" the trace element concentration on the surface determined by the partial adsorption equilibrium. If the diffusion flux is faster than mineral growth rate, the trace element content of the solid will approach that of a solid solution in equilibrium with the aqueous phase.

In other words, the progressing precipitation tends to 'entrap' the composition of surface, whereas the diffusivity drives the sub-surface layer to take a composition closer to that in a (hypothetical) equilibrium between aqueous electrolyte (or melt) and solid solution. With this assumption, it is easy to admit that zoning can occur even at very low growth rates, if the diffusivity is low enough. The sensitive parameter does not seem to be the growth rate alone or the diffusion alone, but the growth rate/diffusivity ratio (Peclet number). Since the mineral continues to grow, the uptake of trace elements in 'older' layers is, in principle, metastable. This irreversible process of enrichment or depletion with trace element relative to the expected aqueous-solid or melt-solid equilibrium concentration is called "surface entrapment".

2.2.1. Enrichment factor

The *enrichment or depletion of Tr* on the surface (adsorbed layer) compared to the bulk of the crystal is described in SEMO by the enrichment factor, *F*:

$$F = \left(\frac{c_{Tr}}{c_{Hc}}\right)_{surface} \Big/ \left(\frac{x_{Tr}}{x_{Hc}}\right)_{bulk,eq} \qquad (2\text{-}6)$$

where *c* stands for the surface (adsorbed) concentration in the appropriate scale. The bulk concentrations correspond to a hypothetical equilibrium between the *Hc*-*Tr* solid solution and the coexisting aqueous solution (or melt). Considering eq (2-2), one can also write:

$$F = \frac{\Delta_{Tr,ads}}{\Delta_{Tr,eq}} \qquad (2\text{-}7)$$

where $\Delta_{Tr,Hc,ads}$ is the fractionation coefficient of the trace element adsorbed on the *Hc* mineral surface, and $\Delta_{Tr,Hc,eq}$ is the equilibrium fractionation coefficient of *Tr* in the solid solution (mineral). In principle, *F* can be obtained from suitable experimental data, or estimated using thermodynamic data: the equilibrium constant ${}^{\Delta}K_{Tr,Hc,eq}$ for the bulk mineral (eq 2-5) and the adsorption constant ${}^{\Delta}K_{Tr,Hc,ads}$, if available. If $F > 1$ then the surface of the mineral is enriched in *Tr* relative to the bulk mineral; if $F < 1$ then the surface is depleted in *Tr*.

The SEMO assumption about the composition of the new layer just after a growth step implies that the subsurface layer is enriched in incompatible trace elements compared to the bulk mineral. At low growth rates, the diffusivity within a nanometre-thick surface layer can adjust the mineral composition to equilibrium with the aqueous solution, hence the measured fractionation coefficient should approach

$\Delta_{Tr,Hc,eq}$. At high growth rates, the diffusivity effect becomes less efficient because the addition of new mineral layers on top of existing ones is much faster, resulting in an increase of $\Delta_{Tr,Hc}$. In other words, there is not enough time for the diffusion process within the top layer to adjust the mineral composition to $\Delta_{Tr,Hc,eq}$. At highest growth rates, the effective $\Delta_{Tr,Hc}$ is expected to approach $\Delta_{Tr,Hc,ads}$. Therefore, the value of the 'phenomenological' fractionation coefficient is confined between $\Delta_{Tr,Hc,eq}$ and $\Delta_{Tr,Hc,ads}$.

Qualitatively, the SEMO appears to explain the variation of $\Delta_{Tr,Hc}$ as a function of the growth rate. However, in order to obtain more quantitative results, some key parameters must be mathematically defined and their values known.

Assuming a constant composition of the aqueous solution, the SEMO computes trace element concentration *C* as a function of depth *h* (*h* = 0 at the surface and decreases with the depth), relatively to C_0, the imaginary aqueous- solid solution equilibrium concentration in the bulk mineral. The initial *Tr* concentration profile was defined by Watson and Liang (1995) as follows:

$$C(h,t=0)=C_0 F^{\exp\left(\frac{h}{l}\right)} \qquad (2\text{-}8)$$

where *l* is the half-thickness of the subsurface layer dominated by adsorption. This assumed exponential decay is a special case of "equilibrium" *Tr* concentration profile that must exist solely due to the fact that the adsorbed concentration of *Tr* in equilibrium with the given aqueous solution is, in general, different from the bulk solid-solution concentration of *Tr* in equilibrium with that aqueous solution.

According to eq. 2-8, the trace metal concentration decreases exponentially from the surface to the bulk mineral. This equation should probably be understood in a sense of mean-field average of the surface composition. Imagine a geometrically ideal surface, perfectly flat. In this case, the *Tr* concentration profile given in the right-hand side of Fig.2 would be a vertical line linking the bulk crystal composition and the surface monolayer composition. However, a crystal surface has kinks, pits, it is never perfectly flat (Sunagawa, 1984; Teng et al., 2000); the adsorption sites are usually heterogeneous (Villieras et al., 2002); and it is shown that the surface structure heterogeneity of calcite determines the surface composition (Paquette and Reeder, 1995). Hence, the real mineral surface is rough and exhibits defects and other heterogeneities. We can imagine roughness as a surface covered by many pits of different size and depth. The deeper from the surface plane the fewer fractions of surface remain exposed in deeper pits; it is reasonable to assume that the exposed surface fraction exponentially decreases toward the bulk mineral. This 'mean-field' decrease is measured by the parameter *l*. It follows from eq (2-8) that when $h < -2l$ then $F^{\exp(-2)}$ approaches unity close enough. Therefore, $2l$ characterizes the effective thickness of the transitional region between the surface and the bulk of the crystal.

2.2.2. Diffusion and diffusivity

The initial SEMO model assumed the diffusion coefficient of *Tr* to be constant through the mineral. In the second version of the model (Watson, 2004), it varies as a function of depth to better fit with experimental results. The empirical expression for the diffusion is:

$$D(h)=D_l\left\{\left(\frac{D_s}{D_l}\right)^{\exp\left(\frac{h}{ml}\right)}\right\} \qquad (2\text{-}9)$$

where D_l is the lattice diffusivity as defined by Cherniak (1997), D_s is the (sub)surface diffusivity, and *m* a multiplier to define the thickness of the high-diffusivity region. Since D_s concerns near-surface regions of the mineral, it cannot be related to the solid-state diffusion like D_l. D_s is simply a way to account for the homogenization of *Tr* concentration in this near-surface layer, a process resembling diffusion and

probably controlled by the fast recrystallization dynamics, reactivity, and heterogeneity of this interfacial region.

There is no direct data on such surface diffusivity so far in the literature, probably due to the fact that such data require accurate solid state analyses at sub-nanometer resolution. Therefore, values of m, l and D_s used in SEMO are usually adjusted using inverse modeling techniques (Tang et al., 2008; Watson, 2004).

2.2.3. Chemical potential

Diffusion is the result of a driving force that can be formulated in terms of chemical potential. When the chemical potential of an element in a phase is different from the chemical potential of this element in another phase, these two phases are considered to be in disequilibrium with respect to each other. Expanding this definition to layers (zones) in the crystal, the expression of the chemical potential of a trace element end member at depth h in the mineral can be written as:

$$\mu(h) = \mu^0 + RT\ln\left[\gamma(h)C(h)\right] \tag{2-10}$$

where μ^0 is the standard-state chemical potential of the trace element end member, R is the universal gas constant, T is the temperature, and γ is the activity coefficient of the trace element end member. In equilibrium, the chemical potential μ_{Tr} should be uniform through the whole mineral and the same in all phases of the system (Fig.2), in spite of the fact that, because of the condition given by eq (2-8), $C(h)$ is not a constant. It is assumed in SEMO (Watson and Liang, 1995) that the variation of C can be accounted for in the activity coefficient term $\gamma(h)$ in eq (2-10):

$$\gamma(h) = \frac{\gamma^0}{F^{\exp\left(\frac{h}{l}\right)}} \tag{2-11}$$

By combining eqs (2-10) and (2-11), one obtains:

$$\mu(h) = \mu^0 + RT\ln\left[\gamma^0 C(h)\right] - RT\exp\left(\frac{h}{l}\right)\ln(F) \tag{2-12}$$

As illustrated in Fig.2, a host mineral growth step buries adsorbed *Tr* ions under a layer of *Hc* component, which results in a shifted *Tr* concentration profile. *Tr* adsorbed on the surface has a different structural environment (and therefore a different Gibbs free energy) than *Tr* buried in the *Hc* crystal lattice; thus, the entrapped *Tr* component exists in a different energetic field and becomes an excess of chemical potential within the sub-surface layer. This local disequilibrium must be compensated via the mass transfer of *Tr* in such a way that the total Gibbs energy is minimized and a uniform, depth-independent profile of μ_{Tr} is restored.

2.2.4. General equation of SEMO

The flux J of the considered trace element trough the mineral is given by Tiller and Ahn (1980):

$$J = -\frac{DC}{RT}\frac{\partial\mu}{\partial h} - VC \tag{2-13}$$

where D is the diffusion coefficient of the trace element trough the mineral (nm^2/s), determined by eq. (2-9), and V is the linear growth velocity (nm/s) of the mineral. The sign of the second term is negative because the growth shifts the coordinate system in such a way that the mineral surface is kept at h=0.

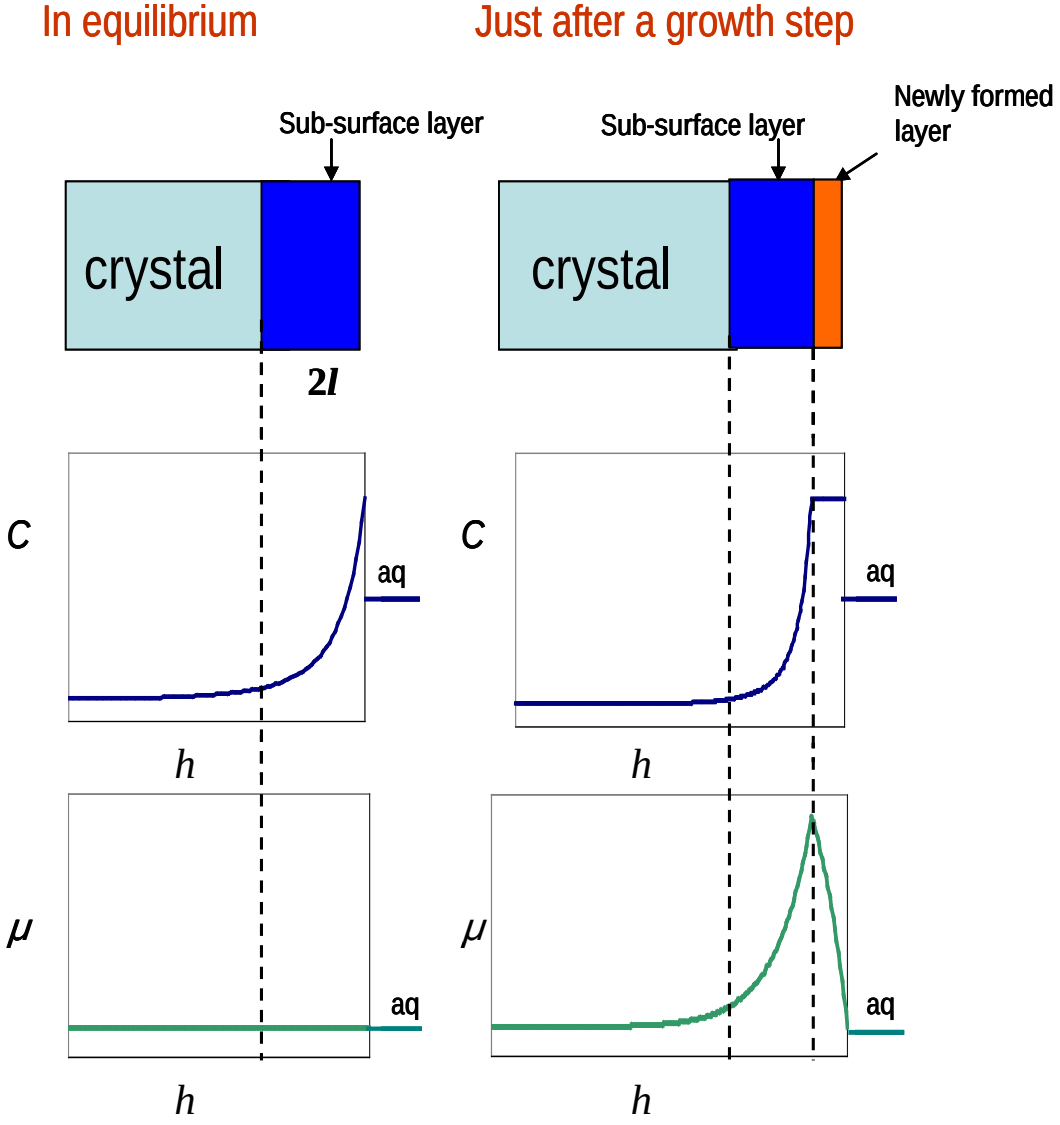

Fig.2: Schematic profiles of relative concentration and chemical potential of an incompatible trace element within a mineral, in equilibrium with the solution, and just after a growth step. From Watson and Liang (1995), modified.

Using the second Fick's law, after some manipulations with derivatives, one obtains the general reactive-transport equation of the SEMO model:

$$\frac{\partial C}{\partial t} = \frac{\partial}{\partial h}\left[D\frac{\partial C}{\partial h}\right] + \left[V - \frac{\ln(F)}{l} D \exp\left(\frac{h}{l}\right)\right]\frac{\partial C}{\partial h} - \frac{\ln(F)}{l} C \exp\left(\frac{h}{l}\right)\frac{\partial D}{\partial h} - D\frac{\ln(F)}{l^2}\exp\left(\frac{h}{l}\right)C \qquad (2\text{-}14)$$

Equations (2-14) and (2-9) can be solved by a Qbasic reactive-transport code (courtesy of E.B.Watson). The code calculates the relative trace-element concentration profile as a function of the depth of the mineral at a given time point. Input parameters are F, V, D_l, D_s, m, l, and the time duration t.

Fig.3 shows examples of modeling using eq (2-14) for compatible and incompatible elements. For an incompatible element with F = 6, after certain growth time, the relative enrichment of the newly grown layer is of factor 4. For a compatible element with F = 0.017, after a certain time, the relative depletion of the newly-grown layer is a factor of 5 relative to the aqueous- solid solution equilibrium concentration.

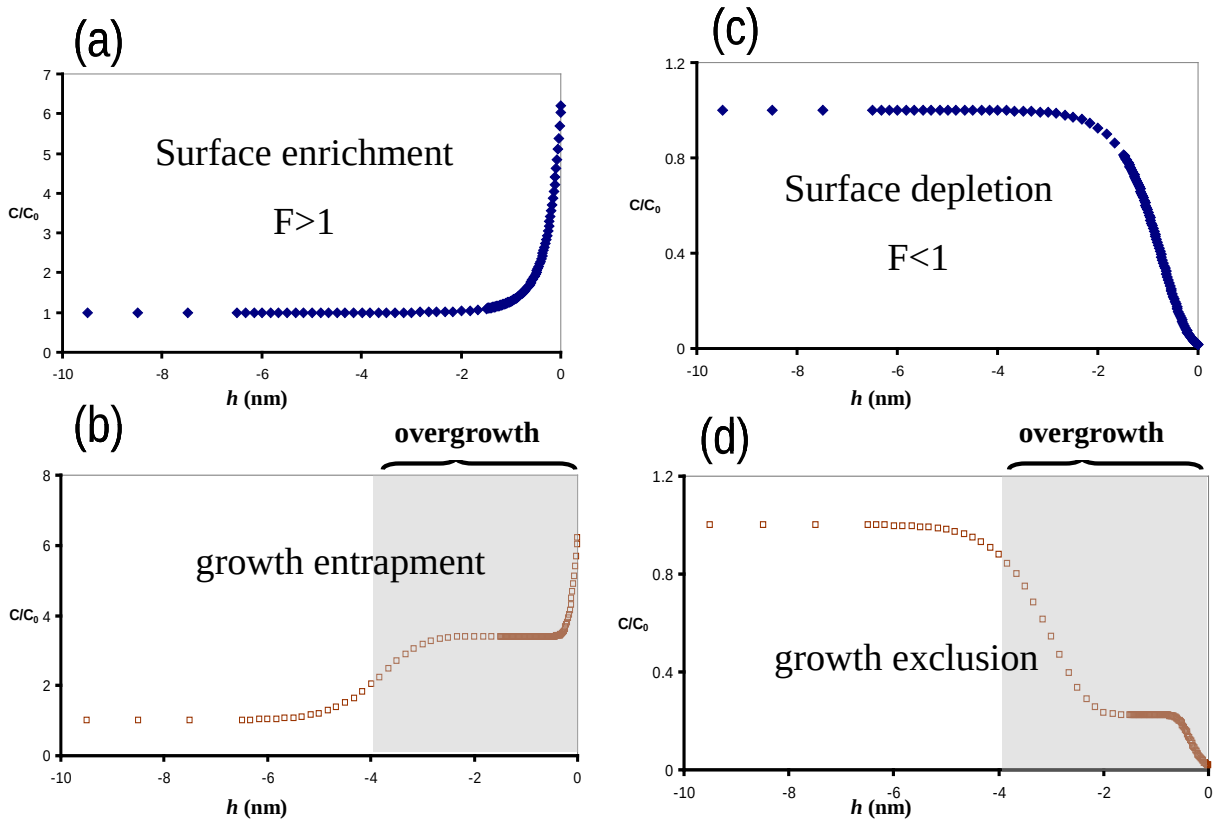

Fig.3: SEMO examples for relative concentration profiles of an incompatible trace element in equilibrium (a) and after growth (b), and of a compatible trace element in equilibrium (c) and after growth (d). (a) and (c) were calculated using eq (2-8), whereas (b) and (d) were obtained using the Q-basic code provided by E.B. Watson. The used parameters were: (b) F=6.2, V=0.08 nm/s, D_s=0.06 nm^2/s, D_l=1.53·10^{-18} nm^2/s, l=0.5 nm, m=6, t=40 s; (d) F=0.017, V=0.0001 nm/s, D_s=0.01 nm^2/s, D_l=1.53·10^{-18} nm^2/s, l=0.5 nm, m=6, t=20000 s.

Note that the kinetic data on mineral precipitation or dissolution rates are usually reported in units of mol/(surface area)/time, whereas V in eqs (2-13, 2-14) is the linear growth velocity in units of distance/time. It can be shown that, assuming spherical shape of particles, the relation between the two kinds of rates is:

$$V = \frac{3M}{\rho} R_p \qquad (2\text{-}15)$$

where V is the linear growth velocity (m/s), M is the molar mass of the host mineral (g/mol), ρ is the host mineral density (g/m^3), and R_p is the precipitation rate (mol/m^2/s). Note that relation (eq 2-15) does not depend on the initial value of the specific surface area of the mineral.

2.2.5. Limitations of SEMO

In reality, especially in (partially) closed systems such as pores in sediments and rocks, V, $\Delta_{Tr,Hc,eq}$ and $\Delta_{Tr,Hc,ads}$ are likely to vary with the aqueous solution composition in time due to reactive-transport effects such as mixing and depletion. The main limitation of SEMO is that the variation of aqueous solution composition and speciation is not accounted for. However, this limitation could be circumvented by embedding SEMO into a geochemical modeling code that can be run sequentially in reaction path calculations.

Another important limitation is that some parameters are not measurable and must be fitted by inverse modeling: the apparent surface diffusivity D_s, the half-thickness of the surface enriched layer l, and the multiplier m linking l to the maximal thickness of the diffusivity region.

At this stage, embedding of the SEMO into a geochemical code appears to be an ultimate condition to improve its usability. In fact, no modification in eqs (2-13, 2-14) will be required to account for variation of F and V because these parameters are fixed in SEMO and do not depend on h, the depth coordinate.

2.3. Surface Reaction Kinetics Model (SRKM)

The Surface Reaction Kinetics Model (DePaolo, 2011) is based on the concept of dynamic precipitation-dissolution close to equilibrium. The model was originally developed to interpret the fractionation of calcium isotopes in calcite, and later on adapted to describe Sr incorporation in calcite.

The Mesoscopic Kinetic Theory (Grmela and Laidlaw, 1983) states that mineral-aqueous equilibrium is a dynamic process, in which precipitation and dissolution rates are equal and compensate each other. In aqueous medium, any mineral is affected simultaneously by a "gross forward precipitation rate" R_f (related to a kinetic rate constant k_f), and a "gross backward dissolution rate" R_b (related to a kinetic constant k_b). The net precipitation rate R_p is the difference between R_f and R_b. For instance, for calcite ($CaCO_3$), R_f and R_b can be related to the activities of ions and the solid in the system (Lopez et al., 2009):

$$R_p = R_f - R_b = k_f (a_{Ca^{2+}})^{n1} (a_{CO_3^{2-}})^{n2} - k_b (a_{CaCO_3})^{n3} \quad (2\text{-}16)$$

where a_i are the species activities, and n_1, n_2, n_3 are the empirical partial reaction order coefficients. R_i and k_i must be expressed in the same units. In equilibrium, R_b is exactly balanced by R_f so that R_p=0.

For the incorporation of a trace cation Tr in calcite, the SRKM equations take the following form:

$$^{Tr}R_f = {}^{Tr}k_f (a_{Tr^{2+}})(a_{CO_3^{2-}}) \quad (2\text{-}17a)$$

$$^{Ca}R_f = {}^{Ca}k_f (a_{Ca^{2+}})(a_{CO_3^{2-}}) \quad (2\text{-}17b)$$

implying $n1 = n2 = 1$. A ratio of rate constants

$$\alpha_f = \frac{{}^{Tr}k_f}{{}^{Ca}k_f} \quad (2\text{-}18)$$

would be sufficient to describe the Tr uptake when only gross forward precipitation rates operate.

For the gross backward dissolution rate:

$$^{Tr}R_b = {}^{Tr}k_b x_{Tr} \quad (2\text{-}19c)$$

$$ {}^{Ca}R_b = {}^{Ca}k_b x_{Ca} \quad (2\text{-}19d) $$

implying $n3 = 1$ and ideal solid solution behavior.

In the same way as eq (2-18), a ratio of backward rate constants can be defined:

$$ \alpha_b = \frac{{}^{Tr}k_b}{{}^{Ca}k_b} \quad (2\text{-}20) $$

This would describe *Tr* uptake in the case when only the gross backward dissolution rate operates. At equilibrium (R_b=R_f), *Tr* uptake is defined by:

$$ \alpha_{eq} = \frac{\alpha_f}{\alpha_b} \quad (2\text{-}21) $$

which is related to *Tr* fractionation coefficient $\Delta_{Tr,Hc}$, as shown below. Combining eq (2-17a), (2-17b) and (2-18) yields:

$$ {}^{Tr}R_f = \alpha_f \, {}^{Ca}R_f \frac{(a_{Tr^{2+}})}{(a_{Ca^{2+}})} \approx \alpha_f \, {}^{Ca}R_f \frac{[Tr^{2+}]}{[Ca^{2+}]} \quad (2\text{-}22) $$

In the same way, one obtains for ${}^{Tr}R_b$:

$$ {}^{Tr}R_b = \frac{\alpha_f}{\alpha_{eq}} {}^{Ca}R_b \left(\frac{x_{Tr}}{x_{Ca}} \right) = \frac{\alpha_f}{\alpha_{eq}} {}^{Ca}R_b \chi_{Tr} \quad (2\text{-}23) $$

where $\chi_{Tr} = x_{Tr} / x_{Ca}$ is denoted for convenience (at trace x_{Tr}, $\chi_{Tr} \approx x_{Tr}$).

Knowing the precipitation and dissolution rates for *Tr* and *Hc*, one can derive the compositional variation of a newly-grown layer surrounding the host mineral (or seed crystal) using the cross-differentiation rules:

$$ \frac{d\chi_{Tr}}{dt} = \frac{1}{x_{Ca}} \left(\frac{d\, x_{Tr}}{dt} - \frac{d\, x_{Tr}}{dt} \chi_{Tr} \right) = \frac{1}{x_{Ca}} \left({}^{Tr}R_p - {}^{Ca}R_p \chi_{Tr} \right) \quad (2\text{-}24) $$

Considering a small time step *dt*, it is reasonable to assume a ‘steady state’ of precipitation (a constant composition of the overgrowth), when

$$ \frac{d\chi_{Tr}}{dt} = 0 \quad (2\text{-}25) $$

By combining eq (2-25) with the r.h.s. of eq (2-24) one obtains:

$$ {}^{Tr}R_p = {}^{Ca}R_p \chi_{Tr} \quad (2\text{-}26) $$

Further, by combining eq (2-26) with eqs (2-16), (2-22) and (2-23) one obtains:

$$ {}^{Ca}R_p = \frac{{}^{Tr}R_p}{\chi_{Tr}} = \frac{{}^{Tr}R_f - {}^{Tr}R_b}{\chi_{Tr}} = \frac{\alpha_f \, {}^{Ca}R_f \frac{[Tr^{2+}]}{[Ca^{2+}]} - \frac{\alpha_f}{\alpha_{eq}} {}^{Ca}R_b \chi_{Tr}}{\chi_{Tr}} \quad (2\text{-}27) $$

Following a tacit assumption by DePaolo (2011), if the amount of trace element is negligible compared to the amount of calcium, then

$$^{Ca}R_p = {}^{Ca}R_f - {}^{Ca}R_b \approx R_f - R_b \quad (2\text{-}28)$$

This assumption is essential for further derivation of the model. By combining eq (2-28) with eq (2-27):

$$\chi_{Tr} = \left(R_f - R_b + \frac{\alpha_f}{\alpha_{eq}} R_b \right) = \alpha_f R_f \frac{[Tr^{2+}]}{[Ca^{2+}]} \quad (2\text{-}29)$$

This can be rewritten as follows:

$$\Delta_{Tr} = \chi_{Tr} \Big/ \left(\frac{[Tr^{2+}]}{[Ca^{2+}]} \right) = \frac{\alpha_f}{1 + \frac{R_b}{R_b + R_p} \left(\frac{\alpha_f}{\alpha_{eq}} - 1 \right)} \quad (2\text{-}30)$$

Eq (2-30) is central in SRKM; it provides the effective value of the fractionation coefficient of a trace element as a function of α_f, α_{eq}, R_p and R_b. This equation means that the value of $\Delta_{Tr,Hc}$ varies between two limits: α_{eq} and α_f. At equilibrium (i.e. $R_p = 0$), $\Delta_{Tr,Hc} = \alpha_{eq}$, whereas at "maximal growth rate" (i.e. $R_b \Rightarrow 0$), $\Delta_{Tr,Hc}$ tends toward α_f (Fig. 4). In other words, there is a growth rate dependency that is qualitatively similar to that produced in the SEMO.

The main advantage of SRKM is that because (eq 2-30) is rather simple, $\Delta_{Tr,Hc}$ can be calculated without a sophisticated computer code. The depletion of *Tr* in aqueous solution can be accounted for sequentially, by considering at each step the growth of a next thin layer. But there are open questions, for instance: how to obtain a proper value of the gross backward dissolution rate R_b, α_f, α_{eq}? Is the concept of gross backward rate R_b physically realistic?

Values of k_b are usually obtained considering dissolution of minerals far from equilibrium (Gudbrandsson et al., 2011; Sidpara and Mehta, 1991; Vavouraki et al., 2010). In this case, according to equation (2-16), the measured backward rate R_b should be equal to the constant $-k_f$. As we know, this may not be quite correct, since the precipitation cannot be considered a reverse of dissolution because of nucleation and Ostwald ripening effects controlling the growth (Fritz et al., 2009). In addition, k_f depends on the solution chemistry, specifically on the ratio $[Ca^{2+}]/[CO_3^{2-}]$ for calcite (Nehrke et al., 2007). Chou et al. (1989) measured a constant $R_b = 6 \cdot 10^{-7}$ mol/m^2/s for pH between 7 and 10 for calcite at 25°C.

Another advantage of the SRKM is its non-sensitivity to the specific surface area effects: R_p and R_b are both normalized to the mineral surface, so whatever the surface area, the R_b/R_p ratio remains the same.

Nielsen et al. (2012) obtained the same equation as eq (2-30), but instead of using gross precipitation and dissolution rates, they considered the kinetics of kink formation and attachment of ions to kink sites. Their work is interesting from the theoretical point of view, although in the practical sense it still requires knowledge of several poorly known additional parameters.

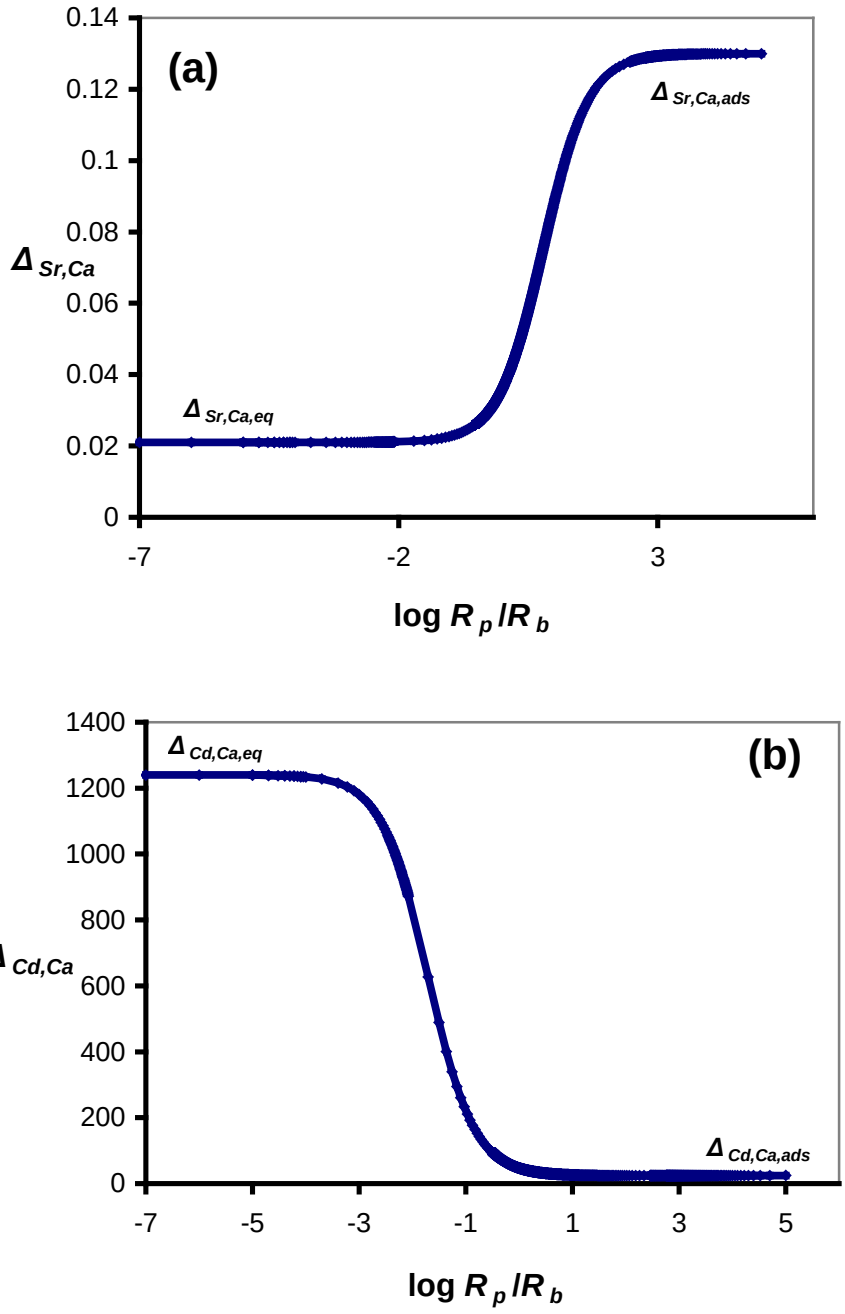

Fig.4: Fractionation coefficient $\Delta_{Tr,Hc}$ in calcite as function of the growth rate, for an incompatible element (a) and a compatible element (b) using $R_b = 6 \cdot 10^{-7}$ mol/m^2/s in both cases. Other SRKM parameters were $\alpha_f = 0.13$ and $\alpha_{eq} = 0.021$ for Sr in calcite, and $\alpha_f = 21$ and $\alpha_{eq} = 1240$ for Cd in calcite.

2.4. Adsorption-Diffusion-Desorption Model (ADDM)

This model was originally proposed by Barrow (1983) to describe sorption and desorption of phosphate by soils. It was later improved in Barrow and Bowden (1987). In the present context, the main assumption of ADDM is that the adsorption or desorption of *Tr* creates a diffusion gradient for sorbed *Tr* to/from the mineral interior. This model does not account for precipitation or dissolution of the host mineral.

The ADDM consists of two parts: adsorption and in-diffusion. At present, the adsorption model part is no longer of interest because several well-developed surface complexation models are available, supported by computer codes (see overview in Kulik, 2009). Nevertheless, we refer here to the Barrow approach in order to help the reader to understand the whole ADDM concept.

In this concept, a simple Freundlich or Langmuir adsorption isotherm is augmented by the account for the impact of variable surface charge. The surface activity a_{is} of a (trace) ion i is given as

$$a_{is} = K_i a_i \exp(-z_i \mathrm{F} \psi_a / RT) \tag{2-31}$$

where K_i is the adsorption constant, and a_i is the activity of i in aqueous solution. The exponential term is, in fact, an activity coefficient where z_i is the adsorbed ion charge, Ψ_a is the relative electrostatic potential of the surface, F is the Faraday constant, R is the universal gas constant, and T is the absolute temperature. If, for instance, the electrostatic potential is negative, it will decrease the adsorption of anions and enhance the adsorption of cations.

The surface activity of i is defined as a Langmuir-isotherm function of the fraction of surface sites θ occupied by i:

$$a_{is} \approx \frac{\theta}{1-\theta} \tag{2-32}$$

By combining eq (2-32) with eq (2-31), one obtains:

$$\theta = \frac{K_i \alpha \gamma c \exp(-z_i F \psi_a / RT)}{1 + K_i \alpha \gamma c \exp(-z_i F \psi_a / RT)} \tag{2-33}$$

where α is the fraction of the free ion in aqueous speciation, (i.e. HPO_4^- / P), γ is the ion aqueous activity coefficient, and c the total molarity of *Tr* in aqueous solution (in mol/L).

Because the absolute electrostatic potential cannot be measured, the relative potential ψ_a must be estimated from the density of adsorbed charge:

$$\psi_a = \psi_{a0} - m_1 \theta - m_2 n(t) / N_m \tag{2-34}$$

where Ψ_{a0} is the reference potential (usually 0), N_m is the maximum amount of surface sites, and $n(t)$ is the amount of ions transferred toward the bulk mineral via diffusion, m_1 and m_2 are empirical parameters. Assuming that the surface concentration $C_{Tr,s} \approx a_{is}$, (only true if $C_{Tr} << C_{Hc}$) the surface amount of adsorbed *Tr* is

$$C_{Tr,s} = N_m \theta \tag{2-35}$$

The increase of the surface activity triggers a diffusion gradient. This is the main difference between ADDM and SEMO, which assumes that surface material is at equilibrium at zero mineral growth rate and thus excludes any macroscopic mass transfer under such conditions. According to Crank (1964), the amount of material transferred to the interior of the mineral (mol/m^2) as function of time and considering a semi-infinite medium is:

$$n(t) = 2 C_{Tr,s} \sqrt{D_k ft / \pi} \tag{2-36}$$

where $C_{Tr,s}$ is concentration of i at the surface of the mineral assumed to be constant (at constant composition of aqueous solution) in mol/m^2, D_k is a coefficient (time^{-1}) (a diffusion coefficient divided by the square of the adsorbed layer thickness), t is the time, and $f = 1/(1-\theta)$ is close to 1 in trace concentration region. In reality, the surface concentration is not necessarily constant, thus, eq (2-36) needs to be integrated over sufficiently small time steps.

The ADDM model allows explaining the frequently observed hysteresis between adsorption and desorption steps. A hysteresis means that the previously sorbed *Tr* amount is not fully desorbed after a certain ageing time. For instance, it was observed and successfully modeled that the longer the ageing time the more pronounced the hysteresis for phosphates on soils (Barrow, 1983) and for Zn on goethite (Barrow et al., 1989) is. Strauss et al. (1997) observed that the higher the specific surface area of goethite the higher the sorption of phosphate, as well as its hysteresis. On "cured" goethites with lower specific surface area (18 m^2/g), nearly all of adsorbed phosphate could be desorbed, whereas only half of the sorbed phosphate could be desorbed from high-surface goethites (132 m^2/g) after a few months ageing, suggesting that the non-desorbed part was retained in the mineral. This kind of retention is explained using ADDM by the diffusion process of adsorbed *Tr* migration into the bulk mineral.

The ADDM only accounts for in-diffusion. The out-diffusion phenomenon is not considered because it can be neglected for relatively short desorption times. In contrast, SEMO accounts for diffusion in both directions. For long simulation times and changing chemical conditions, accounting for out-diffusion may be important. Out-diffusion could, for instance, take place after a desorption event due to a change of the solution pH. Such an improvement is manageable using a reactive-transport code. In any case, a reactive-transport code must be used to simultaneously solve eqs (2-33) to (2-36).

At constant surface concentration, (eq 2-36) provides the amount of material transferred towards the bulk mineral per unit surface area as a function of diffusion coefficient and time. If diffusion of sorbed ions towards the bulk mineral occurs indeed, this model would be able to explain the observed hysteresis between sorption and desorption e.g. through the fraction of desorbed material:

$$f_{desorbed} = \frac{C_{Tr}}{C_{Tr} + n(t)} \qquad (2\text{-}37)$$

Using (eq 2-37), we modeled the desorption experiments of Cd on goethite (Mustafa et al., 2006) and of Cs on illite (de Koning and Comans, 2004). We adjusted the D_k parameter at values at 0.02 s^{-1} and 6 s^{-1}, respectively. Note for comparison, that D_k = 0.007 s^{-1} for Cd in calcite considering D_s and l parameters used in section 3.1.2. Larger specific surface areas of goethite and illite and their surface roughness might explain the higher values of the apparent diffusivity coefficient. Fig.5 shows that this simple model fits well with the experimental data. So, modeling in-diffusion of adsorbed ions toward the bulk mineral is at least consistent with the observed hysteresis between adsorption and desorption.

Another observation is that the larger the specific surface area *Ss* the higher the surface diffusivity seems to be. Considering that $C_{Tr,s}$ is not related to the *Ss*, the *Ss* effects may be implicitly included in the parameter D_k. A higher *Ss* implies a more efficient *Tr* flux toward the interior of the mineral. A mathematical link between D_k and *Ss* or surface roughness is not yet properly established and needs further investigations.

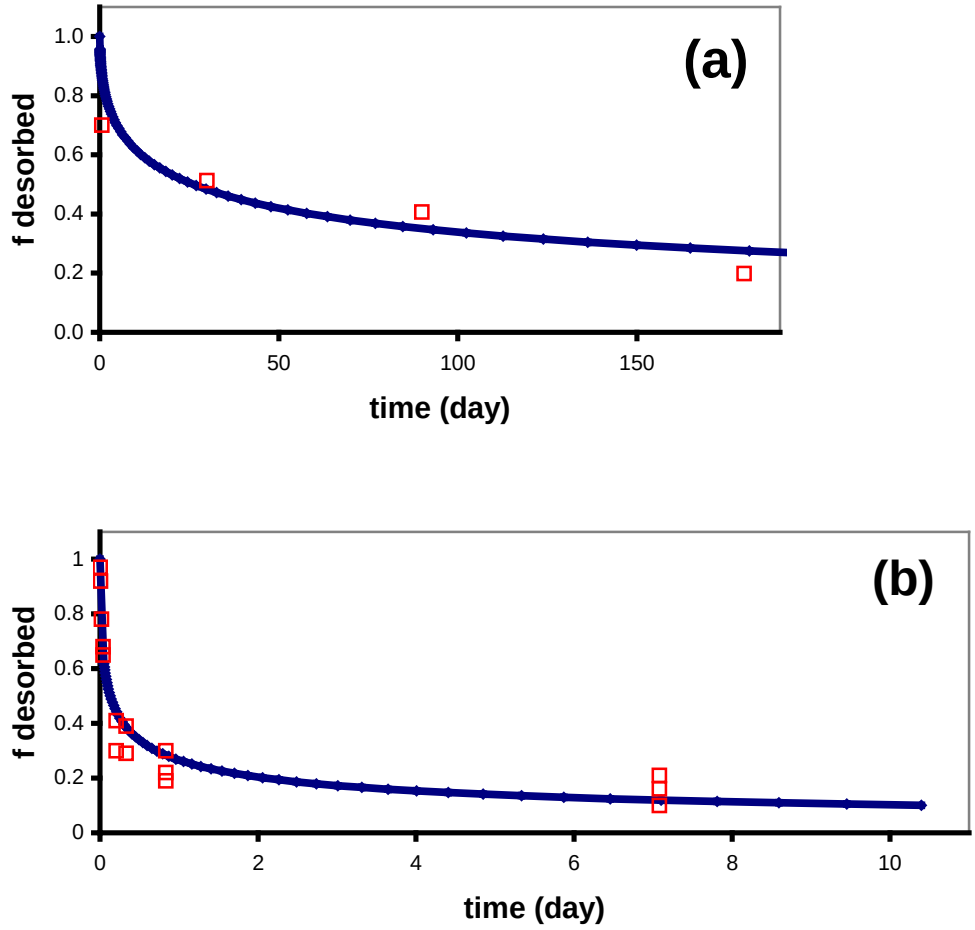

Fig.5: Fraction of desorbed material for Cd in goethite (a) and Cs in illite (b). Curves are modeling results obtained using a simplified version of ADDM, whereas scattered symbols are experimental data from Mustafa et al. (2006) and De Koning and Comans (2004), respectively.

Compared to other two models, the limitation of the ADDM is that the growth of the mineral is not considered. In addition, the diffusion is only allowed into the bulk mineral. In contrast, the SEMO considers diffusion/diffusivity both into and out of the mineral, whereas the SRKM does not explicitly consider diffusion or diffusivity-related processes.

In/out diffusion effects may be very relevant for the long-term processes in SKIN context, where they cannot be ignored.

2.5. Gibbs Energy Minimization (GEM)

GEM finds equilibrium phase assemblage and speciation vector $n^{(x)}$ in the system (GEM primal solution) defined by T, P, vector of bulk composition of the system $n^{(b)}$, standard molar Gibbs energies of all components in all phases g^o, and parameters of mixing and non-ideality in solution phases. Simultaneously, GEM calculates the chemical potentials of elements and charge (GEM dual solution vector u) (Kulik et al., 2012; http://gems.web.psi.ch).

In more formal terms, GEM minimizes the total Gibbs energy of the system computed from species amounts and primal chemical potentials:

$$G(n^{(x)}) \Rightarrow \min \quad s.t. \quad \mathrm{A}n^{(x)} = n^{(b)} \tag{2-38}$$

where $n^{(x)} \geq 0$ and $\mathrm{A} = \left\| a_{ij} \right\|$ is the stoichiometry matrix made of formulae of j-th chemical species (dependent component) expressed in mole amounts of i-th element (independent component).

Within the common mass balance $\mathrm{A}n^{(x)} = n^{(b)}$, metastabilities can be enforced as the non-trivial non-negativity constraints from below $\underline{n}_j$ and/or from above $\overline{n}_j$ on the sought-for amount of any j-th chemical species $n_j^{(x)}$. In the case of mineral, constraining its amount from below can be used for simulating dissolution, and from above, to simulate precipitation (growth).

Achievement of the equilibrium state is checked using the Karush-Kuhn-Tucker necessary and sufficient conditions that compare dual and primal GEM solutions:

$$\begin{aligned} &\upsilon - \mathrm{A}^T u \geq 0; \\ &\mathrm{A}\hat{n}^{(x)} = n^{(b)}; \quad \hat{n}^{(x)} \geq 0; \\ &\hat{n}^{(x)}\left(\upsilon - \mathrm{A}^T u\right) = 0 \end{aligned} \tag{2-39}$$

where the elements of vector υ are the normalized primal chemical potentials of j-th species:

$$\upsilon_j = g_j^o / RT + \ln C_j + \ln \gamma_j + \Xi \tag{2-40}$$

calculated, as usual, from the concentration $C_j = f(\hat{n}_j^{(x)}, \hat{n}^{(x)})$ and activity coefficient γ_j (Ξ stands for molality conversion terms). We see that in eq (2-39), primal chemical potentials are actually compared with their dual-solution counterparts,

$$\hat{\eta}_j = \sum_{i \in N} a_{ij} \hat{u}_i \tag{2-41}$$

For any stable chemical species, $\upsilon_j = \hat{\eta}_j$ (in practice, equal to numerical precision). If non-trivial metastability constraints are present then the extended form of conditions (2-39) is used (details in Kulik et al., 2012).

Not far from equilibrium, kinetic rate laws contain the affinity term (1 - Ω_k), based on the k-th mineral stability (or saturation) index Ω_k. In the GEM algorithm, Ω_k of any compound or phase is computed in a simple and general way from GEM dual solution:

$$\Omega_k = \sum_{j \in l_k} \exp\left(\hat{\eta}_j - \frac{g_j^o}{RT} - \ln \gamma_j - \Xi_k \right) \tag{2-42}$$

where the index *j* runs over all end-members (components, species) comprising the phase.

The stability criterion for any phase used in GEM algorithm is based on its logarithmic stability index $\log_{10}\Omega_k$. If $\log_{10}\Omega_k$ = 0(numerically) then the phase is in equilibrium with the rest of the system. If $\log_{10}\Omega_k < 0$ then the phase is unstable (undersaturated), but may be kept in mass balance by metastability constraint(s) $\underline{n}_j$ set at least on one of its components. If $\log_{10}\Omega_k < 0$ then the phase is overstable (the rest

of the system is oversaturated relative to this phase) because metastability constraint(s) from above $\overline{n}_j$ is set at least on one of its components.

Taken together, the output phase stability index Ω_k together with the input additional lower- $\underline{n}_j$ and upper $\overline{n}_j$ constraints make the GEM-Selektor code a versatile tool for modeling various kinds of kinetics and metastability, represented as sequences of partial (constrained) equilibrium states (Kulik et al., 2012a)).

3. First results and discussion

3.1. Comparison between SEMO and SRKM

Comparative modeling exercises were performed for Sr and Cd in calcite at 25°C, the systems where the most experimental data were available.

3.1.1. Sr in calcite

Considering an equilibrium fractionation coefficient in the bulk mineral of $\Delta_{Sr,Ca,eq}$ = 0.021 (Tesoriero and Pankow, 1996) and a sorption fractionation coefficient of $\Delta_{Sr,Ca,ads}$ = 0.13 (Zachara et al., 1991), one obtains the enrichment factor F=6.2, which we used in our modeling. Note that in the case of the fastest growth rates, experimental $\Delta_{Sr,Ca}$ barely exceed the value of 0.13 (Huang and Fairchild, 2001; Lorens, 1981; Tang et al., 2008; Tesoriero and Pankow, 1996) most probably corresponding to the surface adsorption, which corroborates consistency of the experimental data.

For SEMO calculations, we took parameter values suggested by Watson (2004): l = 0.5 nm, m = 6 and D_s = 0.060 nm^2/s. The lattice diffusivity $D_l = 1.53 \cdot 10^{-18}$ nm^2/s was taken from Cherniak (1997).

In SRKM calculations, we obtained the best fit to experimental data with $R_b = 7 \cdot 10^{-8}$ mol/m^2/s.

We did not succeed to model the experimental results of Gabitov and Watson (2006) measured at very high growth rates, 1 to 4 orders of magnitude greater than those in other experiments. In this data, incorporation of Sr continues to increase as function of V to about factor 3 of the maximum value of 0.13 from sorption and other coprecipitation experiments. This kind of Sr "super-enrichment" might be the result of fluid inclusions entrapment or of the precipitation rate being higher than the adsorption reaction rate.

As seen on Fig.6a, both SEMO and SRKM predict similar trends and describe qualitatively the experimental results, although the slopes are not the same. Significant deviations between the data and the model curves are observed, in particular, for the data of Tesoriero and Pankow (1996).

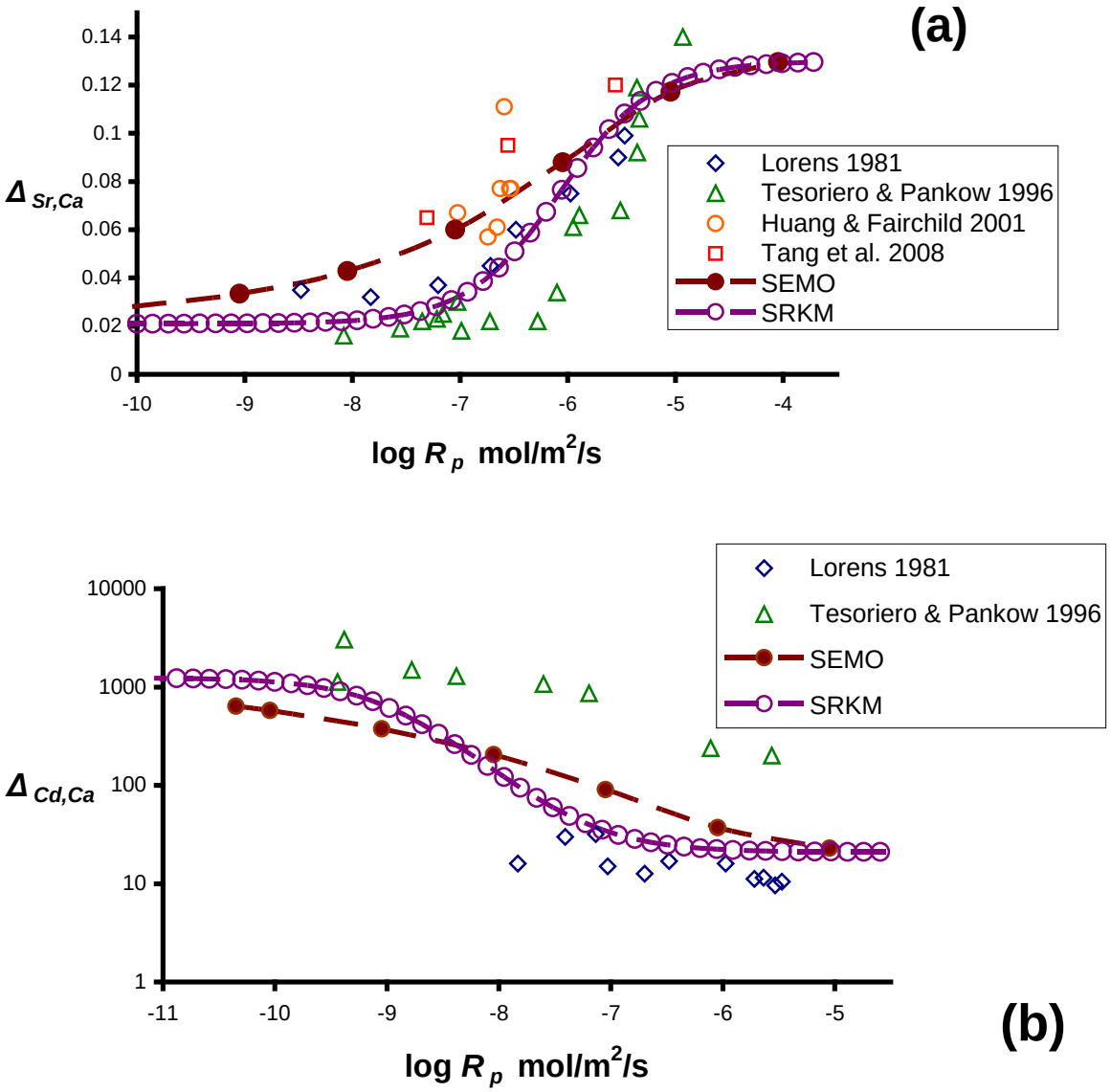

Fig.6: Comparison between SEMO, SRKM predictions (curves) and experimental data for calcite: $\Delta_{Sr,Ca}$ (a) and $\Delta_{Cd,Ca}$ (b).

3.1.2. Cd in calcite

Using experimental data (Tesoriero and Pankow, 1996; Zachara et al., 1991), we have calculated the enrichment factor F=0.017 in the same way as done before for Sr in calcite. For the SEMO, we took D_s = 0.017 nm^2/s measured for calcite by Ahmed et al. (2008) while keeping the previously mentioned values of m and l. We did not change the value of D_l, although the diffusion coefficients are not expected to be the same for Sr^{2+} and Cd^{2+} due to the different ionic radii. In any case, the effect of D_l variation is negligible compared to that of D_s: a D_l variation of 1 order of magnitude had no effect on entrapment model curve. For the SRKM, we used $R_b = 3 \cdot 10^{-8}$ mol/m^2/s.

Comparison between experiment and modeling is given in Fig.6b. To obtain optimal fits to both experimental datasets, it is not possible to use the same value of $\Delta_{Cd,Ca,eq}$. The reason is probably that the aqueous chemistry is not the same: pH, Cl concentration, and ionic strength are quite different, as well as methods used to calculate fractionation coefficients. Contrary to Sr, Cd is sparingly soluble and forms complexes which may lead to different fractionation coefficients if they are defined based on total element concentrations. This example highlights that the implementation of uptake kinetics models in a geochemical code is necessary.

3.2. Merging the models

The experimental data can be modelled reasonably well with both SEMO and SRKM. The common outcome from both models is that the fractionation coefficient $\Delta_{Tr,Ca}$ varies between two limits, $\Delta_{Tr,Ca,eq}$ and $\Delta_{Tr,Ca,ads} = F \cdot \Delta_{Tr,Ca,eq}$. This suggests that SRKM might be considered as an integrated form of SEMO (which is a reactive transport model), and raises the question whether the two uptake models could be merged into a generalized one, ideally having the physics of SEMO and the simplicity of the SRKM.

In both concepts, high precipitation rates constrain the composition of the newly grown incremental layer, with *Tr* content greater than expected from Aq-SS equilibrium if *Tr* is incompatible with the host mineral structure ($F > 1$), and less than that, if *Tr* is compatible ($F < 1$). This enrichment or depletion can be counterbalanced by a release of entrapped *Tr* back to aqueous solution. This release is assigned to a dissolution phenomenon in SRKM and to an out or in-diffusion phenomenon in SEMO, although it must not necessarily be regarded as a "true" diffusion phenomenon.

According to Fick's laws, the existence of a concentration gradient (or chemical potential) of *Tr* element between two points triggers a diffusion flux of *Tr* in direction of lower concentration or potential, until re-equilibration is achieved. Diffusion occurring inside a mineral is commonly called "solid state or lattice diffusion", which is denoted in SEMO with the symbol D_l. Since D_l is extremely low compared to the sub-surface diffusivity D_s and laboratory time scales are much lower than the time needed for lattice diffusion to proceed significantly, a variation of D_l by one order of magnitude has no influence on the entrapment. Its effect can thus be neglected at laboratory time scales, so an accurate value of this parameter is not required in such conditions. On the contrary, the surface diffusivity D_s is a critical parameter, which is unfortunately hard to determine experimentally. Most probably, D_s does not represent a real diffusion process, but rather a transfer of elements resulting from dissolution/ reprecipitation phenomena occurring at the mineral-water interface, enhanced by surface roughness.

As discussed in section (2.2.1), the exponential decrease of trace element content with depth assumed in SEMO in equilibrium, can be related to surface roughness and heterogeneity, measured by the *l* parameter in the mean-field sense.

Considering that the surface diffusivity is due to the dynamics of the rough surface, the SEMO concept appears to be not really so different from the SRKM. Hence, as a first hypothesis we assumed that the R_b in SRKM is playing a similar role as D_s in SEMO, namely controls the (backward) transport of elements from the surface layer of the mineral to the aqueous solution.

We propose to consider in SEMO the quantity V_b (in m/s), which can be regarded as a 1-D analogue of the surface diffusivity:

$$V_b = \frac{D_s}{ml} \tag{3-1}$$

where *ml* is the length in which the surface diffusivity occurs, as defined before. *V* and V_b are dimensionally consistent; they can be compared more obviously than *V* and D_s, like R_p and R_b can be compared in the SRKM. Considering that the same phenomenon triggers D_s and R_b, we further assume:

$$\frac{R_b}{R_p} = \frac{V_b}{V} \tag{3-2}$$

Combining eq (2-30) with eqs (3-2,3-1) leads to:

$$\Delta_{Tr,Hc} = \frac{F \cdot \Delta_{Tr,Hc,eq}}{1 + \frac{\left(\frac{D_s}{ml}\right)}{\left(\frac{D_s}{ml}\right) + V}(F-1)} \tag{3-3}$$

This equation has mathematical form similar to eq (2-30) and is able to yield a very similar curve shape. A limitation of this merged model is that the lattice diffusion (present in SEMO and, as in-diffusion parameter, in the ADDM) is not accounted for, although, at very long reaction time, the effect of lattice diffusion may be significant. Further improvement of the merged model should account for the in-diffusion phenomenon.

3.3. Current implementation in GEM-Selektor

A realistic simulation has to account for the aqueous speciation because the equilibrium fractionation coefficient $\Delta_{Tr,Hc,eq}$ can vary as a function of aqueous solution composition. Aqueous speciation can also influence the growth rate, which, in addition, may depend on depletion effects in closed systems. To account for these effects, the merged uptake kinetics model (eq. 3-3) was implemented as a process simulation script in the GEM-Selektor v.3.1 package that uses the GEM algorithm (Kulik et al., 2012), see section 2.5.

The idea was to simulate the time evolution of the system using a sequence of partial equilibrium states controlled by additional lower- $\underline{n}_j$ and/or upper $\overline{n}_j$ metastability constraints on two end-members as function of time according tokinetic rate laws. The metastability constraint $\overline{n}_{Cal}$ on calcite end-member is calculated via a usual kinetic precipitation rate, whereas metastability constraints $\underline{n}_{Tr} = \overline{n}_{Tr}$ on *Tr* end-member are calculated from the current amount of calcite $\overline{n}_{Cal}$ using eq (3-3). This flow diagram is shown in Fig.7.

At each time step, the current amount of precipitated mineral is calculated using a kinetic law. For calcite, we have chosen the empirical law by Wolthers et al. (2012):

$$V_{Cal} = I^{-0.004}\, pH^{-10.71} \cdot \left(\frac{a_{Ca^{2+}}}{a_{CO_3^{2-}}}\right)^{-0.35} \cdot (\Omega^{0.5} - 1)^2 \tag{3-4}$$

where I is the ionic strength of the solution, and Ω is the calcite saturation index. Like other kinetic equations, this one considers the saturation index as a driving force; the maximum rate is achieved at about equal activities of Ca^{2+} and CO_3^{2-} ions in aqueous solution. The obtained growth velocity V_{Cal} is converted into the R_p scale using eq (2-15).

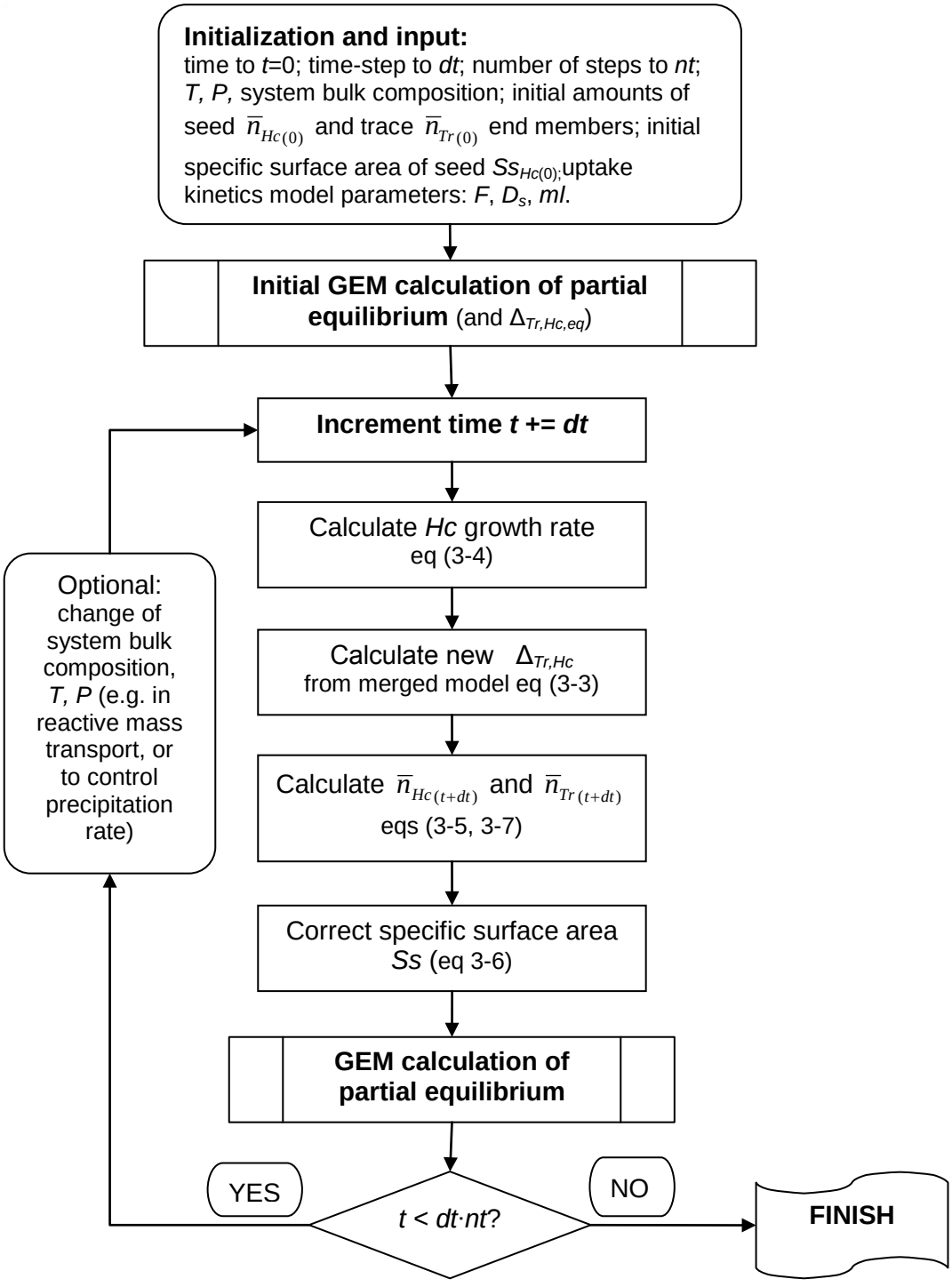

Fig. 7: Flow-chart showing the implementation of uptake kinetics as a reaction-path simulation in GEM-Selektor.

Now, the metastability constraint $\overline{n}_{Cal}$ (mol) can be calculated using the precipitation rate $R_{p,Cal}$, the mineral specific surface area Ss_{Cal}, and the time step dt. At each time step, the increment value (which corresponds to the mole amount precipitated during the time-step) is added:

$$\overline{n}_{Cal(t)} = n_{Cal(t-1)} + Ss_{Cal(t-1)} \cdot M_{Cal} \cdot n_{Cal(t-1)} R_p \cdot dt \qquad (3\text{-}5)$$

where $\overline{n}_{Cal(t)}$ is the amount constraint on calcite at time t, and $n_{Cal(t-1)}$ is the amount of calcite from the previous time step (or at t=0 during the first time-step).

Mineral surface area is expected to vary during the growth process. Considering a spherical growth model, the Ss variation can be expressed as:

$$Ss_{Cal(t)} = Ss_{Cal(0)} \left(\frac{\overline{n}_{Cal(0)}}{\overline{n}_{Cal(t)}} \right)^{\frac{1}{3}} \qquad (3\text{-}6)$$

where $Ss_{Cal(0)}$ is the initial specific surface area (m^2/g), $\overline{n}_{Cal(t)}$ is the current amount of calcite, and $\overline{n}_{Cal(0)}$ is the initial amount of the mineral (mol).

The next step is to obtain the metastability constraint on the Tr end-member, as follows:

$$\overline{n}_{Tr(t)} = \overline{n}_{Tr(t-1)} + (\overline{n}_{Cal(t)} - n_{Cal(t-1)}) \cdot \Delta_{Tr,Ca} \frac{[Tr^{2+}]_{(t-1)}}{[Ca^{2+}]_{(t-1)}} \qquad (3\text{-}7)$$

This equation is strictly valid when $x_{Tr} << x_{Ca}$. $\Delta_{Tr,Ca}$ is calculated using the merged model (eq 3-3). The equilibrium partition coefficient, $\Delta_{Tr,Ca,eq}$, necessary to calculate $\Delta_{Tr,Ca}$, is obtained via an aqueous- solid-solution model (Kulik et al., 2010). For Sr-calcite, the regular interaction parameter W_G = 4400 J/mol was used. Note that $\Delta_{Tr,Ca,eq}$ is not updated at every time step, but calculated only at t=0 and assumed to be constant throughout the process simulation.

3.4. Modeling examples

The merged uptake model (eq 3-3) implemented in GEM-Selektor as described in the previous section was used to model the coprecipitation experimental data on Sr and Cd uptake by calcite (Lorens, 1981).

The chemical thermodynamic system was set up in stoichiometry basis C, Ca, Cd, Cl, N, H, Na, O, Sr, charge. The list of phases and involved components, with thermodynamic data taken from GEM-Selektor variant of Nagra-PSI data base (Hummel et al. 2002) is provided in Appendix B for the user's convenience. Aqueous activity coefficients were calculated using the Debye-Hückel equation.

Results are presented on Fig.8. For each experimental point, a full sequential GEM-Selektor calculation was performed from t=0 to the relevant maximum time of reaction. Modeling points shown represent the last time-step (corresponding to the full reaction time in each experiment) and are connected by a curve for clarity. $\Delta_{Tr,Ca}$ is a global fractionation coefficient integrated over the total amount of precipitated mineral, i.e. it corresponds to the average composition of the overgrowth. Because R_p is not always perfectly constant during the simulation process, the average value of R_p (sum of each value divided by the number of time steps) was calculated and presented in Fig.8.

Plotted $\Delta_{Tr,Ca}$ were not directly those calculated with eq (3-3), but were recalculated using eq (2-2.b).As we can see, there is a good correlation between experimental data and modeling results, indicating that our tool may be appropriate to describe the growth-rate dependency of the fractionation coefficient, both for compatible or incompatible elements.

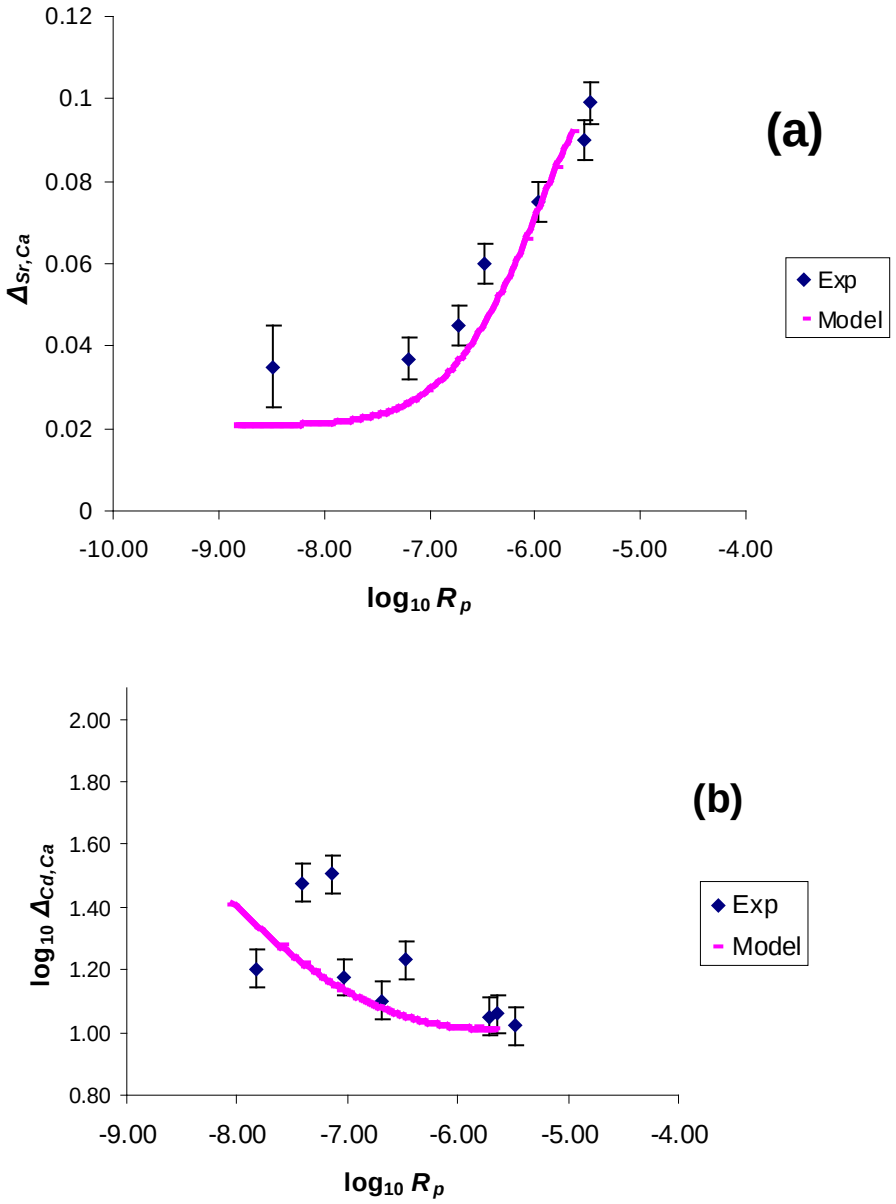

Fig.8: Fractionation coefficient as a function of growth rate R_p (mol/m^2/s) in $\log_{10}$ scale for Sr in calcite (a) and Cd in calcite (b). Curves: our 'merged' uptake kinetics model calculated in GEM-Selektor simulations; scattered symbols are experimental data (Lorens, 1981).

Implementation of the "merged model" in GEM-Selektor framework can be a useful tool to interpret specific experimental results, allowing the growth-rate dependency of fractionation coefficients to be considered in complex geochemical models together with changes in aqueous solution composition. In this way, the depletion effects can be accounted for with their impact on *Hc* precipitation rate and, further, on fractionation coefficients. Such modeling can be verified against experimentally calibrated systems, similar to Sr and Cd uptake in calcite used here as an example, even though the aqueous composition barely changes in such experiments. Further, the reaction path algorithm such as shown on Fig. 7 can be

applied to closed or semi-closed systems where significant depletion is expected, e.g. pore spaces in rocks or cement, where the advection-diffusion transport occurs.

To verify our reaction path simulations to other *Tr*/*Hc* systems, relevant experimental data are necessary. Ideally, a data set of co-precipitation experiments conducted at different growth rates would allow to extract required parameters and to calibrate the model for the considered *Tr/ Hc* couple in the mineral of interest.

4. Difficulties encountered during the first reporting period

- Doubts concerning the typographical correctness of specific equations and assumptions made in the relevant theoretical papers. In the case of SEMO, we could circumvent such problems, as we were able to use the original Q-basic code that Professor E.B.Watson kindly provided us with.

- Issues in reconciling different available experimental datasets, which necessitates conversions to the same units of measurement (i.e. growth rate that can be expressed in m/s, mol/m^2/s, mol/s/g seed, etc) and to consistent parameter definitions (e.g. partition, distribution, fractionation coefficients).

- Insufficiency of the available experimental data for testing the uptake kinetics models. Complete data sets exist only for Sr and Cd in calcite. Lacking information on the chemical system may prevent its implementation in GEM-Selektor modeling projects. For instance, it was not yet possible to model some data from (Tesoriero and Pankow, 1996) because the initial mass of seed crystal and the amount of added material could not be found in that publication.

5. Conclusions and perspectives

Three uptake kinetics models from the literature were evaluated: the growth Surface Entrapment Model (SEMO), the Surface Reaction Kinetic Model (SRKM), and the Adsorption-Diffusion-Desorption Model (ADDM). All of them are able to qualitatively describe time-dependent uptake of trace elements in host minerals.

SEMO and SRKM were merged into a 'generalized' model to make it usable in a geochemical modeling code. The ADDM was not yet included because it does not consider mineral growth. Nevertheless, the in-diffusion phenomenon accounted for in ADDM can have a relevant effect for long-term uptake processes. Further consideration of ADDM may thus help understand the relations between specific surface area and sub-surface diffusivity.

The merged model of trace element uptake in growing solid solution minerals can be used to describe experimental results at various deviations from equilibrium. The growth-rate dependency of trace element fractionation coefficients appears to be well described: for structurally incompatible elements (e.g. Sr in calcite) the fractionation coefficient increases with increasing mineral growth rate, whereas for compatible elements (e.g. Cd in calcite), the fractionation coefficient decreases with increasing growth rate. These rate effects are typically less than an order of magnitude.

More accurate knowledge of some relevant parameters (e.g., D_s, R_b) would be necessary in order to obtain robust modeling results (i.e. "blind predictions" instead of multiple parameter fitting). Unfortunately, obtaining such parameters experimentally would require sophisticated techniques (nm-resolution mapping, kinetic experiments) and a major effort from the side of experimentalists.

Specifically, the following experimental or estimated data are necessary to further test the discussed uptake models:

(1) Thermodynamic data for solid solution end members and non-ideality of mixing for the considered trace/host element couple, in order to calculate $\Delta_{Tr,Hc,eq}$;

(2) The value of $\Delta_{Tr,Hc,ads}$ for the adsorption of trace element on host mineral, or an adsorption model that can yield it, to determine the enrichment factor *F*;

(3) Precipitation and dissolution kinetic rate laws for the host mineral, applicable over *pH* and *I* ranges of interest;

(4) Value of the sub-surface diffusivity D_s for the considered couple trace element/mineral, as a function of specific surface area. Potentially, this parameter can be estimated from AFM and other data on surface roughness and dynamics, or found by inverse modeling or uptake kinetic data;

(5) Experimental co-precipitation dataset (with known variation of the growth rate) for trace element in host mineral, to verify the uptake kinetics model.

In the framework of SKIN project, further improvement of our 'merged' model of uptake kinetics will consist in the implementation of in-diffusion as described in the SEMO and in the ADDM, which can influence $\Delta_{Tr,Hc}$ especially at long time scales.

The effect of specific surface area or surface roughness on sub-surface diffusivity parameter seems to be essential, as indicated by the positive correlation between specific surface area and sub-surface diffusivity. This suggests that a high specific surface area of the host mineral may lead to faster uptake of trace element. This issue certainly deserves more investigation, both experimental and theoretical.

For reaction-path modeling of time-dependent uptake using the 'merged' model, as implemented in GEM-Selektor package, more scoping calculations need to be done in order to determine the effect of changing time step value on modeling results. The impact of time stepping is a key issue in reactive-transport modeling in general.

'Hard-coding' of the developed uptake kinetics model into a built-in subroutine is necessary to make such models usable in geochemical reactive-transport codes coupled with the GEMS3K kernel of GEM-Selektor package.

References

Ahmed, I. A. M., Crout, N. M. J., and Young, S. D., 2008. Kinetics of Cd sorption, desorption and fixation by calcite: A long-term radiotracer study. *Geochimica et Cosmochimica Acta* **72**, 1498-1512.

Barrow, N. J., 1983. A mechanistic model for describing the sorption and desorption of phosphate by soils. *Journal of Soil Science* **34**, 733-750.

Barrow, N. J. and Bowden, J. W., 1987. A comparison of models for describing the adsorption of anions on a variable charge mineral surface. *Journal of Colloid and Interface Science* **119**, 236-250.

Barrow, N. J., Gerth, J., and Brummer, G. W., 1989. Reaction-kinetics of the adsorption and desorption of nickel , zinc and cadmium bu goethite .2. Modeling the extent and rate of reaction. *Journal of Soil Science* **40**, 437-450.

Cherniak, D. J., 1997. An experimental study of strontium and lead diffusion in calcite, and implications for carbonate diagenesis and metamorphism. *Geochimica et Cosmochimica Acta* **61**, 4173-4179.

Chou, L., Garrels, R. M., and Wollast, R., 1989. Comparative study of the kinetics and mechanisms of dissolution of carbonate minerals. *Chemical Geology* **78**, 269-282.

Crank, J., 1964. The Mathematics of Diffusion. Oxford University Press, Oxford.

de Koning, A. and Comans, R. N. J., 2004. Reversibility of radiocaesium sorption on illite. *Geochimica et Cosmochimica Acta* **68**, 2815-2823.

DePaolo, D. J., 2011. Surface kinetic model for isotopic and trace element fractionation during precipitation of calcite from aqueous solutions. *Geochimica et Cosmochimica Acta* **75**, 1039-1056.

Fritz, B., Clement, A., Amal, Y., and Noguera, C., 2009. Simulation of the nucleation and growth of simple clay minerals in weathering processes: The NANOKIN code. *Geochimica et Cosmochimica Acta* **73**, 1340-1358.

Gabitov, R. I. and Watson, E. B., 2006. Partitioning of strontium between calcite and fluid. *Geochem. Geophys. Geosyst.* **7**, 12.

Gamsjager, H., Preis, W., Konigsberger, E., Magalhaes, M. C., Brandao, P., 1999. Solid-solute phase equilibria in aqueous solution. XI. Aqueous solubility and standard Gibbs energy of cadmium carbonate. *Journal of Solution Chemistry* **28**, 711-720.

Grmela, M. and Laidlaw, W., 1983. Mesoscopic kinetic theory. *Journal of. Chem. Phys*. **78**, 5151.

Gudbrandsson, S., Wolff-Boenisch, D., Gislason, S. R., and Oelkers, E. H., 2011. An experimental study of crystalline basalt dissolution from 2 <= pH <= 11 and temperatures from 5 to 75 degrees C. *Geochimica et Cosmochimica Acta* **75**, 5496-5509.

Huang, Y. and Fairchild, I. J., 2001. Partitioning of Sr^{2+} and Mg^{2+} into calcite under karst-analogue experimental conditions. *Geochimica et Cosmochimica Acta* **65**, 47-62.

Hummel , W., Berner, U., Curti, E., Pearson, F.J., and Thoenen, T., 2002. Nagra/PSI Chemical Thermodynamic Data Base 01/01. Universal Publishers, Parkland, Florida.

Kulik, D.A., 2009: Thermodynamic concepts in modeling sorption at the mineral-water interface. In: Thermodynamics and Kinetics of Water-Rock Interactions (Eds. E.H.Oelkers, J.Schott), Reviews in Mineralogy and Geochemistry 70, 125-180.

Kulik, D. A., Vinograd, V. L., Paulsen, N., and Winkler, B., 2010. (Ca,Sr)CO_3 aqueous-solid solution systems: From atomistic simulations to thermodynamic modelling. *Physics and Chemistry of the Earth, Parts A/B/C* **35**, 217-232.

Kulik, D.A., Thien, B., and Curti, E., 2012a. Partial-equilibrium concepts to model trace element uptake. *Goldschmidt'2012 Conference Abstract, Montreal.*

Kulik, D.A., Wagner, T., Dmytrieva, S.V., Kosakowski, G., Hingerl, F.F., Chudnenko, K.V., and Berner U. (2012): GEM-Selektor geochemical modeling package: Numerical kernel GEMS3K for coupled simulation codes. *Computational Geosciences* (in press), doi: http://dx.doi.org/10.1007/s10596-012-9310-6.

Lopez, O., Zuddas, P., and Faivre, D., 2009. The influence of temperature and seawater composition on calcite crystal growth mechanisms and kinetics: Implications for Mg incorporation in calcite lattice. *Geochimica et Cosmochimica Acta* **73**, 337-347.

Lorens, R. B., 1981. Sr, Cd, Mn and Co distribution coefficients in calcite as a function of calcite precipitation rate. *Geochimica et Cosmochimica Acta* **45**, 553-561.

Mustafa, G., Kookana, R. S., and Singh, B., 2006. Desorption of cadmium from goethite: Effects of pH, temperature and aging. *Chemosphere* **64**, 856-865.

Nehrke, G., Reichart, G. J., Van Cappellen, P., Meile, C., and Bijma, J., 2007. Dependence of calcite growth rate and Sr partitioning on solution stoichiometry: Non-Kossel crystal growth. *Geochimica et Cosmochimica Acta* **71**, 2240-2249.

Nielsen, L. C., DePaolo, D. J., and De Yoreo, J. J., 2012. Self-consistent ion-by-ion growth model for kinetic isotopic fractionation during calcite precipitation. *Geochimica et Cosmochimica Acta* **86**, 166-181.

Paquette, J. and Reeder, R. J., 1995. Relationship between surface structure, growth mechanism, and trace element incorporation in calcite. *Geochimica et Cosmochimica Acta* **59**, 735-749.

Shock, E. L., Sassani, D. C., Willis, M., and Sverjensky, D. A., 1997. Inorganic species in geologic fluids: Correlations among standard molal thermodynamic properties of aqueous ions and hydroxide complexes. *Geochimica et Cosmochimica Acta* **61**, 907-950.

Sidpara, G. R. and Mehta, B. J., 1991. Gross dissolution of natural rhombohedral-shaped calcite in glacial acetic-acid. *Cryst. Res. Technol.* **26**, 875-881.

Strauss, R., Brummer, G. W., and Barrow, N. J., 1997. Effects of crystallinity of goethite .2. Rates of sorption and desorption of phosphate. *Eur. J. Soil Sci.* **48**, 101-114.

Sunagawa, I., 1984. Growth of crystals in nature. In: Sunagawa, I.(Ed.), Material Science of the Earth's Interior. Terra Scientific Publishing, Tokyo.

Tang, J., Köhler, S. J., and Dietzel, M., 2008. Sr^{2+}/Ca^{2+} and $^{44}Ca/^{40}Ca$ fractionation during inorganic calcite formation: I. Sr incorporation. *Geochimica et Cosmochimica Acta* **72**, 3718-3732.

Teng, H. H., Dove, P. M., and De Yoreo, J. J., 2000. Kinetics of calcite growth: surface processes and relationships to macroscopic rate laws. *Geochimica et Cosmochimica Acta* **64**, 2255-2266.

Tesoriero, A. J. and Pankow, J. F., 1996. Solid solution partitioning of Sr^{2+}, Ba^{2+}, and Cd^{2+} to calcite. *Geochimica et Cosmochimica Acta* **60**, 1053-1063.

Thien B., Kulik D.A., and Curti, E., 2012. Adding uptake kinetics and surface entrapment to geochemical models. *Goldschmidt'2012 Conference Abstract, Montreal.*

Tiller, W. A. and Ahn, K. S., 1980. Interface field effects on solute redistribution during crystallization. *Journal of Crystal Growth* **49**, 483-501.

Vavouraki, A. I., Putnis, C. V., Putnis, A., and Koutsoukos, P. G., 2010. Crystal growth and dissolution of calcite in the presence of fluoride Ions: An atomic force microscopy study. *Cryst. Growth Des.* **10**, 60-69.

Villieras, F., Michot, L. J., Bardot, F., Chamerois, M., Eypert-Blaison, C., Francois, M., Gerard, G., and Cases, J. M., 2002. Surface heterogeneity of minerals. *C. R. Geosci.* **334**, 597-609.

Watson, E. B., 2004. A conceptual model for near-surface kinetic controls on the trace-element and stable isotope composition of abiogenic calcite crystals. *Geochimica et Cosmochimica Acta* **68**, 1473-1488.

Watson, E. B. and Liang, Y., 1995. A simple model for sector zoning in slowly grown crystals; implications for growth rate and lattice diffusion, with emphasis on accessory minerals in crustal rocks. *American Mineralogist* **80**, 1179-1187.

Wolthers, M., Nehrke, G., Gustafsson, J. P., and Van Cappellen, P., 2012. Calcite growth kinetics: Modeling the effect of solution stoichiometry. *Geochimica et Cosmochimica Acta* **77**, 121-134.

Zachara, J. M., Cowan, C. E., and Resch, C. T., 1991. Sorption of divalent metals on calcite. *Geochimica et Cosmochimica Acta* **55**, 1549-1562.

Appendix A

List of symbols

A	stoichiometry matrix made of formulae of chemical species
(a_i)	activity of i-th aqueous species;
a_{is}	surface activity of the i-th ion;
C	relative trace element concentration of tracer in the host mineral;
C_o	imaginary aqueous-solid solution equilibrium concentration of tracer in the host mineral;
C_j	concentration of element j in its phase;
$C_{Tr,s}$	constant concentration of *Tr* at the surface of the mineral, in mol/m^2 ;
c	total molarity of dissolved (*Tr*) in aqueous solution, in mol/L;
c_i	surface (adsorbed) concentration of the i-th species in the appropriate scale;
$D(h)$	diffusivity coefficient as function of depth, in nm^2/s;
D_k	coefficient related to the diffusion coefficient via the thickness of the adsorbed layer, in s^{-1};
D_l	lattice diffusion coefficient, in nm^2/s;
D_s	surface diffusivity, in nm^2/s;
dt	time-step, in s;
F	Faraday constant, 96485.3 C/mol;
F	enrichment factor for a given trace element in a given host mineral;
$f_{desorbed}$	fraction of desorbed component;
$G(n^{(x)})$	total Gibbs energy of the system;
g_j^o	standard molar Gibbs energy function of a component j;
h	depth from surface in the host mineral, in nm;
$[i]$	molarity of the i-th chemical species or component in mol/L;
I	ionic strength of aqueous solution, in mol/L or molality units
J	flux of the considered trace element trough the host mineral;
K_i	adsorption constant of i-th species;
${}^{\Delta}K_{Tr}$	fractionation constant of a trace element *Tr* between aqueous solution and a mineral;
${}^{\Delta}K_{Tr,eq}$	equilibrium value of K_{Tr} ;
k_b	gross backward dissolution constant of the host mineral, in mol/m^2/s;
k_f	gross forward precipitation constant of the host mineral, in mol/m^2/s;
${}^{i}k_b$	gross backward dissolution constant of *i*–th end-member, in mol/m^2/s;
${}^{i}k_f$	gross forward precipitation constant of *i*–th end-member, in mol/m^2/s;
l	half-thickness of the surface enriched layer, in nm;

M	molar mass of the considered host mineral, in g/mol;
m	multiplier to define the width of the high diffusivity region;
m_1	adjustable parameter;
m_2	adjustable parameter;
N_m	maximum amount of adsorbed ions (mol);
$n^{(b)}$	vector of bulk composition of the system;
$n^{(x)}$	equilibrium phase assemblage and speciation vector in the system (GEM primal solution);
$n(i)$	amount of precipitated end-member i or host-mineral i, in mol;
$n(i)_0$	initial amount of precipitated end-member i, or host-mineral i, in mol;
$n(t)$	amount of ions transferred toward the bulk mineral via diffusion, in mol/m^2;
$\underline{n}_j$	additional metastability constraint on j-th component amount from below;
$\overline{n}_j$	additional metastability constraint on j-th component amount from above;
$n_j^{(x)}$	sought-for amount of j-th component (chemical species) in GEM primal solution;
$\hat{n}_j^{(x)}$	amount of j-th component (chemical species) in equilibrium;
$\hat{n}^{(x)}$	final (equilibrium state) vector of mole amounts of all components in the system;
pH	pH of aqueous solution;
R	universal gas constant, 8.31451 J/K/mol;
R_b	gross backward dissolution rate, in mol/m^2/s;
R_f	gross forward precipitation rate, in mol/m^2/s;
R_p	net precipitation rate of the considered host mineral, in mol/m^2/s;
${}^iR_b$	gross backward dissolution rate of i–th end-member, in mol/m^2/s;
${}^iR_f$	gross forward precipitation rate of i–th end-member, in mol/m^2/s;
Rd	distribution ratio;
S	surface area of the host mineral, in m^2;
Ss	specific surface area of the host mineral, in m^2/g;
Ss_0	initial specific surface area of the host mineral, in m^2/g;
T	temperature, in K;
t	time, in s;
V	unidimensional mineral face growth rate (orthogonal to surface), in nm/s;
V_b	unidimensional gross backward dissolution rate of the mineral, in nm/s;
V_{cal}	unidimensional growth rate of calcite host mineral, in m/s;
z_i	change of the adsorbed ion;
α	fraction of the free ion in aqueous speciation;

α_{eq} equilibrium fractionation ratio;

α_f fractionation ratio in the case of maximal growth rate;

$\Delta_{Tr,Hc}$ fractionation coefficient of a given trace element between aqueous solution and mineral;

$\Delta_{Tr,Hc,ads}$ fractionation coefficient of a trace element adsorbed on surface of the host mineral;

$\Delta_{Tr,Hc,eq}$ fractionation coefficient of a trace element *Tr* in the considered host solid solution;

γ_i activity coefficient of i-th species or component;

$\mu(h)$ chemical potential of the trace element end member;

μ^0 standard-state chemical potential of the trace element end member;

Ξ conventional terms such molality conversion;

θ fraction of occupied surface sites;

ρ density of the considered host mineral, in g/m^3;

υ vector of primal chemical potentials of dependent components (species)

υ_j normalized primal chemical potential of j-th species;

x_i mole fraction of the i-th chemical species or component;

χ_{Tr} molar fraction of the *Tr* element in the host mineral;

Ψ_a relative electrostatic potential of the surface (adsorption layer);

Ψ_{a0} reference electrostatic potential of the surface (adsorption layer);

Ω saturation index of the mineral (relative to aqueous solution);

Ω_k stability index of *k*-th phase in GEM algorithm.

Appendix B

Chemical thermodynamic system used in GEM-Selektor calculations of Sr and Cd uptake in calcite at *T*=25 C, *P* = 1 bar.

Species	G^{o}_{298}
Ca(CO3)@	-1099176
Ca(HCO3)+	-1146041
Ca+2	-552790
CaOH+	-717024
Cd+2	-77655
CdCl+	-220191
CdCl2@	-355017
CdCl3-	-485223
CdCl4-2	-611203
CdO2-2	-281583
CdO2H-	-361916
CdO@	-198740
CdOH+	-257316
Na(CO3)-	-797112
Na(HCO3)@	-847394
Na+	-261881
Sr+2	-563836
CO3-2	-527982
HCO3-	-586940
Cl-	-131290
H2@	17729
N2@	18194
O2@	16446
OH-	-157270
H+	0
H2O@	-237181
CO2,gas	-394393
H2,gas	0
N2,gas	0
O2,gas	0
Calcite CaCO3	-1129176
Otavite CdCO3	-674200
Sr-calcite SrCO3	-1135000
Strontianite SrCO3	-1144735

G^{o}_{298}, the Gibbs energy of formation from elements in their standard states, in J/mol. '@' means 'neutral'. Sources: GEMS version of Nagra-PSI 01/01 database (Hummel et al., 2002); SUPCRT92 database for Cd aqueous species (Shock et al., 1997); (Gamsjager et al., 1999) for otavite).

Regular interaction parameter W_G (J/mol) for solid solutions

Calcite - Sr-Calcite	Calcite - Otavite
4400	2974.8
Kulik et al., 2010	This work

Kinetic parameters used in modeling exercise Fig.6.

Parameter	Sr in calcite	Cd in calcite
F	6.2	0.3
D_l (nm^2/s)	$1.53 \cdot 10^{-18}$	$1.53 \cdot 10^{-18}$
D_s (nm^2/s)	0.06	0.017
l (nm)	0.5	0.5
M	6	6